Daik et al., J Material Sci Eng 2015, 5:2
DOI: 10.4172/2169-0022.1000222

Journal of Material Sciences & Engineering

Research Article Open Access

Application of Gettering Process on the Improvement of the Structural and Mineralogical Properties of Tunisian Phosphate Rock

Daik R[1]*, Lajnef M[2], Amor SB[1], Elgharbi S[3], Meddeb H[1], Abdessalem K[4], Férid M[3] and Ezzaouia H[1]

[1]*Photovoltaic Laboratory Research and Technology Centre of Energy, Borj-Cedria Science and Technology Park, BP 95, 2050 Hammam-Lif, Tunisia*
[2]*Sfax Preparatory Engineering Institut, Route Menzel Chaker, 0.5 km, BP 1172, 3080 Sfax, Tunisia*
[3]*National Research Center in Sciences of Materials, Borj-Cedria Science and Technology Park, B.P. 95 Hammam-Lif, 2050, Tunisia*
[4]*L3M, Department of Physics, Faculty of Sciences of Bizerte, 7021 Zarzouna, Tunisia*

Abstract

The present study deals with the effects of gettering process on the structural and mineralogical composition of Tunisian phosphate rock. The treated samples were characterized to investigate the variation of physical structure and chemical composition as compared to the reference phosphate rock. The quantitative analysis of the impurities concentration before and after gettering treatment using energy-dispersive (EDX) reveals a significant reduction of impurity concentration (more than 75%) such as Al, Si, S, Na, and Mg. Scanning electron microscopy (SEM) shows that gettering process promoted structural alterations of phosphate rock sample due to fusion of impurities. The XRD patterns show that the chief mineral constituent of treated sample is only fluorapatite, while those in the reference ore were calcite, dolomite, quartz and carbonate-fluorapatite. FT-IR characterization show a disappearance of the bands related to calcite at 714 cm^{-1} as well as B carbonate situated at 1430 cm^{-1}, 1458 cm^{-1} after gettering treatment. This result is in good correlation with Raman analysis.

Keywords: Phosphate rock; Gettering; Impurities; Structure

Introduction

Gafsa which is located in the south of Tunisia is one of the largest phosphate producers in the word (more than 10 million tons per year since the early nineties) [1]. The phosphate rock is used to manufacture phosphate fertilizers and industrial products and, also the only significant global resource of phosphorus used in animal feed supplements, food preservatives, anti-corrosion agents, cosmetics, fungicides, ceramics, water treatment and metallurgy [2]. The rock is composed essentially of the apatite group in association with a wide assortment of accessory minerals mainly fluorides, carbonates (calcite and/or dolomite), clays, quartz, silicates, metal oxides as well as organic matters and trace impurities such as U, REEs (rare earth elements), Cd, As, V, Cr, Zn, Cu, Ni, etc., which can be harmful for several application at certain concentration [3-6].

Gettering process typically consists on a combined a rapid thermal treatment (RTP) followed by a chemical etching after the growth of a porous layer in order to reduce impurities amount and to enhance the phosphate quality. The rapid thermal treatment aims to migrate the impurities to the boundaries surface where they undergone an elimination process by a chemical attack.

The gettering treatment is an effective process to eliminate these impurities which was already applied in our laboratory for the purification of silica [7]. Although, characterization and quantification of the impurities contained in Tunisian phosphate is well established, there are not many reports about their elimination and phosphate purification [5,8-12]. In the present work, we aim not only to improve the structural and mineralogical properties but also to eliminate the majority of these impurities contained in Tunisian phosphate by gettering treatment. The changes in physical structure and chemical composition of the samples after gettering treatment have been investigated by using X-ray powder diffraction (XRD), scanning electron microscopy (SEM/EDX), FT-IR, and Raman spectroscopies. Transmission electron microscope (TEM) micrographs were performed to inspect the morphological properties after treatment.

Materials, Procedure and Methods

Materials

Phosphate rock samples used in this study was obtained from the phosphate deposits from the Metlaoui basins located in the south of Tunisia. It was crushed, ground, and then sieved, the fraction in the range between 180 µm and 600 µm was used. This fraction was crushed by a jaw breaker, reaching a dimension of to 180 µm. Another manual grinding is performed using an agate mortar in order to increase specific surface area.

Procedure

The experimental procedure consists in two steps:

First step (formation of porous layer): the porous layer of phosphate rock is formed by CAVP technique (Chemical Attack in the Vapor Phase) when the sample is exposed to an acidic vapor composed of 64% HNO_3, 20% CH_3COOH and 16% HF. The vapor phase etching is performed under heating at 45°C for 60 minutes. The objective of growing of porous layer on the grain surface is to increase the specific surface layer, thus the impurities can be removed easily.

Second step (gettering process): the sample of porous phosphate is introduced in the rapid thermal furnace (RTP) at a fixed temperature 900°C for 45 minutes under a flow of oxygen. In order to remove the impurities from the samples, the thermally treated porous phosphate undergoes four iterative etchings: 1 g of the former sample is etched

***Corresponding author:** Daik R, Photovoltaic Laboratory Research and Technology Centre of Energy, Borj-Cedria Science and Technology Park, BP 95, 2050 Hammam-Lif, Tunisia, Tel: 21655303006; E-mail: daik.ridha.crten@gmail.com

Received November 30, 2015; **Accepted** December 14, 2015; **Published** January 04, 2016

Citation: Daik R, Lajnef M, Amor SB, Ezzaouia H, Elgharbi S, Meddeb H, et al. (2015) Application of Gettering Process on the Improvement of the Structural and Mineralogical Properties of Tunisian Phosphate Rock. J Material Sci Eng 5: 222. doi:10.4172/2169-0022.1000222

with 20 ml of diluted solution of CP4 (3 ml HCl + 1 ml HNO_3 were dissolved in 996 ml of deionizer water). The mixed solution undergoes a stirring for 3 minutes. The treated phosphate in the final phase is separated from the obtained solution by a filtration system of 0.54 mesh diameter. The solid remaining was washed, dried during 1 hour at 100°C then weighed with a precision. For simplification, we have noted (RP) the reference phosphate sample and (TP) phosphate after gettering treatment (treated phosphate).

Methods

X-Ray diffraction were performed using X'PERT Pro Philips analytical diffractometer operating at wavelength Kα copper (λ = 1.5418 nm) and the obtained results were analyzed using the software X'PertisHigh Score Plus.

The IR spectra were recorded using a Nicolet 560 spectrometer; samples pelletized using a pressein potassium bromide (KBr) to 2 mg of product 300 mg of KBr. Registration is realized in the range between 4000 cm^{-1} and 400 cm^{-1}.

Raman shift were recorded with micro-Raman spectroscopy (Jobin Yvon Horibra LABRAMHR) in 400 cm^{-1}-1100 cm^{-1} range. The excitation source was 632.8 nm line of He-Ne laser. The microstructure of samples was characterized by transmission (Technai G2) electron microscopy. The chemical composition was determined by energy diserive X-ray EDX analysis. For the TEM sample preparation, we employed the ultrasound vibration method [13]. The samples were immersed in ethanol solution and ultrasound vibration was applied to separate precipitates from the phosphate. After that, the precipitates were carefully extracted in the solution and picked up using TEM copper meshes with carbon film coatings.

Results and Discussion

XRD characterization

A powder X-ray diffraction (XRD) analysis was used to determine the crystalline phases of the Tunisian natural phosphates rocks before and after getting process. The XRD patterns of the treated phosphate rocks as well as the raw material are illustrated in Figure 1.

The main minerals in reference phosphate rocks (RP) are carbonate-fluorapatite (2θ: 25.99°; 28.17°; 29.44°; 31.97°; 33.24°; 34.15°; 40.31°; 42.48°; 44.48°; 47.01°; 49.55°; 50.81°; 53.09°) (JCPDS 00-021-0141),

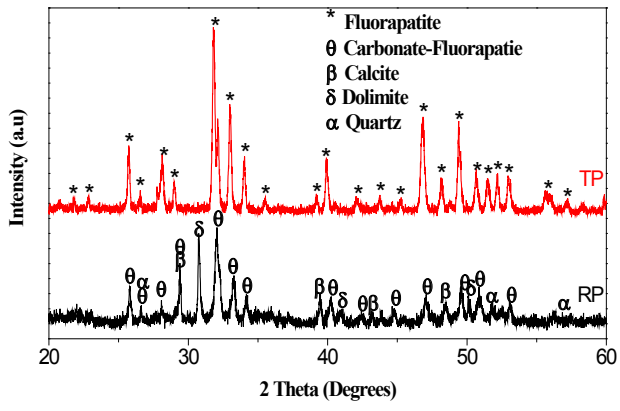

Figure 1: Diffractogramms of the reference phosphate (RP) and the treated phosphate (TP).

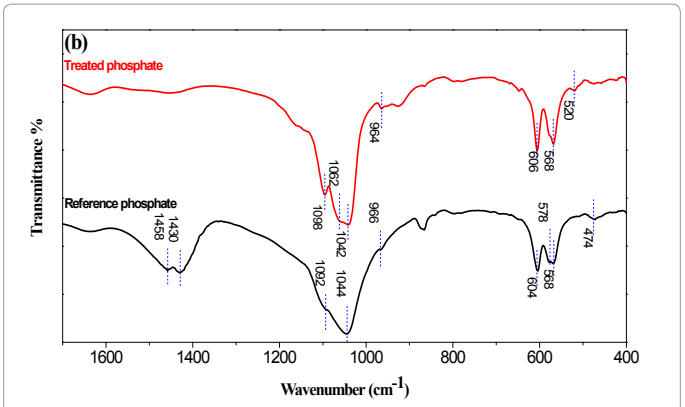

Figure 2: FT-IR spectrum of Tunisian phosphate rock before (RP) and after treatment (TP).

quartz SiO_2 (2θ: 26.54°; 51.9°; 56.25°) (JCPDS 01-080-2146), carbonates which are in the form of dolomite CaMg $(CO_3)_2$ (2θ : 30.7°, 41.06°, 50.09°) (JCP¨DS 01-073-2409) and calcite $CaCO_3$ (2θ : 29.44°, 39.42°, 43.18° and 48.46°) (JCPDS 01-072-1652). Calcite and quartz were the main gangue minerals in the Tunisian phosphate rock. Concerning the treated sample (TP), as expected from Figure 1, the major crystalline phase is hexagonal fluorapatite (FAp) ($Ca_{10}(PO_4)6F_2$), space group $P6_3/m$ (JCPDS 01-079-1459). The highest intensity near 33° confirms the fluorapatite behavior of the treated sample [2,7,9,10,14,15].

Calcite and quartz diffraction lines are disappeared as a result of gettering process, also carbonate-fluorapatite has changed to fluorapatite because carbonates are decomposed by rapid thermal treatment. Therefore, it was proved in others works that rapid thermal treatment at 900°C leads to a phosphate with relatively higher P_2O_5 and CaO contents and a disappearance of organic matter [16,17]. In this work CaO formed after rapid thermal treatment was eliminated by chemical attack in vapor phase (ACPV).

XRD pattern of treated phosphate compared with reference sample (Figure 1) shows a good resolution of the peaks and a decrease of the width at half maximium which proves an amelioration of crystalinity after gettering process.

X-ray diffraction analysis indicates that certain level of impurities were removed during gettring process of phosphate rock. However, the improvement of the phosphate quality of treated sample depends on the mass percentages of the remaining impurities, notably the quartz, calcite and dolomite. In previous work, it was demonstrated also that the reduction of phosphate impurities was associated with some structural changes in the apatite [16].

FT-IR characterization

Figure 2 shows the FT-IR spectra of Tunisian phosphate before and after gettering treatment in the region of 4000 cm^{-1}-400 cm^{-1}. From this figure, we can observe that the gettering process had a remarkable an important effect on the vibrational bands intensity and its positions; also we can note the appearance and disappearance of some pics.

The FTIR spectrum indicates that the reference phosphate rock spectrum shows that the characteristic absorption bands corresponds to the carbonate fluorapatite [7,17,18]. The symmetric υ1 (stretching) mode assigned to PO_4^{3-} is represented by a single band at 966 cm^{-1}. The υ2 (bending) mode of phosphate groupment is located at 474 cm^{-1}. The strong absorption band at 1044 cm^{-1} ascribed to asymmetric υ3

mode. The asymmetric υ4 mode is splited in three bands: 568, 578 and 604 cm^{-1}. The two bands at 1430 cm^{-1} and 1458 cm^{-1} were assigned to υ2 vibration of CO_3^{2-} group located in the B site of apatite (carbonate substituting phosphate) [17]. The spectrum of main component of the phosphate rock reference sample is in a good agreement with published IR spectra of apatite [19-21].

FT-IR spectra of the TP sample illustrated in Figure 2 reveals that the vibrational bands of treated phosphate were clearly observed compared with reference phosphate rock. The absorption peaks located at 1098 cm^{-1} and 1062 cm^{-1} originated from asymmetrical stretching υ3 of PO_3^{-4} and the peaks localized at 568 cm^{-1} and 606 cm^{-1} were attributed to bending modes υ4 of PO_3^{-4}. While the symmetric stretching modes υ1 and υ2 of PO_3^{-4} were also observed at around 964 cm^{-1} and 520 cm^{-1} respectively [21].

Moreover, after gettering process, the band positions and their intensities are slightly affected and we observe a change in the number of phosphate bands, the treated phosphate indicates that the bands at 520 cm^{-1} corresponding to υ2 strongly shifted from 474 cm^{-1} to 520 cm^{-1}. Concerning the shift, it can be due to the variation repulsion potential of the contracted or dilated crystal lattice which is confirmed by XRD analysis [7,22]. The positions of υ4 and υ1 modes didn't change but an important increase of intensity was marked. The υ3 asymmetric mode was degenerated in tow distiguitched peacks at 1042 cm^{-1} and 1062 cm^{-1}. The appearance of the two distinct peaks is due to the presence of different P-O distances in the crystal.

Besides, a considerable reduction in the absorption of carbonate bending is shown clearly after gettering treatment. In fact, we remark a disappearance of the bands related to calcite at 714 cm^{-1} as well as B carbonate situated at 1430 cm^{-1}, 1458 cm^{-1}. This implies that carbonate and calcite substitutions induce vacancies at the OH sites, and we assume that thermal treatment is responsible of the total decomposition of carbonate bands and intensities decreases [23]. Thus, the results indicate that mixture acids can be used to reduce calcium carbonate in low-grade calcareous phosphate rock as it improves the degree of beneficiation [24].

RAMAN characterization

Raman scattering is a sensitive tool for studying the phosphate material because it gives direct structural evidence qualitatively related to the different components in the material. Figure 3 shows the Raman spectra for RP and TP. From this figure, we can't observe any vibrational mode for reference sample (RP). This is due to the fact that Raman bands are completely overlapped by the fluorescence background originated from organic matter, metal compouned and rare earth existing in natural phosphate rock (RP) [25-29]. As a result of this overlap, we can't differentiate between the different vibrational modes.

For the TP, Raman spectra shows obviously the different vibrational modes of phosphates groupement after Gettering process. The strongest Raman active υ1 of PO_3^{-4} mode appearance in the spectrium of the TP sample at 961 cm^{-1} [30,31].

To better clarify the vibrationnal modes existing in TP, deconvolution of the Raman spectrum were shown in Figures 4 and 5. The Raman spectrum of phosphate in the 125-300 cm^{-1} spectral range is illustrated in Figure 4. Raman bands are observed at 139, 169, 214, 234, 265 and 283 cm^{-1}. These bands are assigned to lattice vibrations as it was reported by many authers [11,18,32].

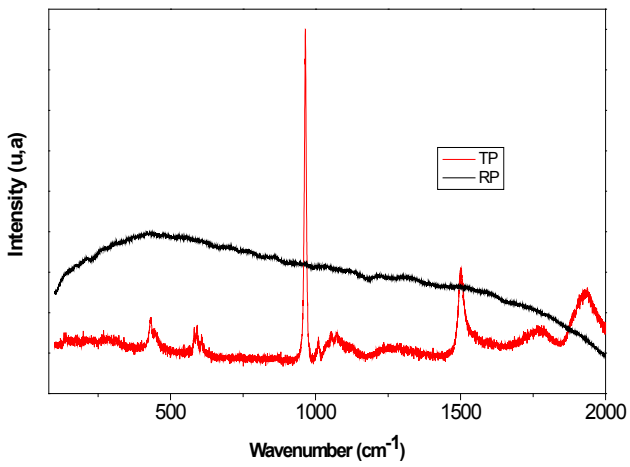

Figure 3: RAMAN spectrum of Tunisian phosphate rock before (RP) and after treatment (TP).

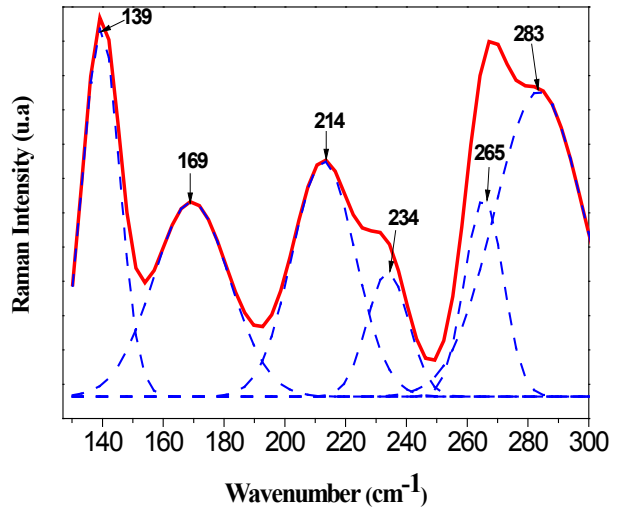

Figure 4: Raman spectrum of treated phosphate over the 125 cm^{-1}-300 cm^{-1} spectral range.

The Raman spectrum of treated phosphate over the 400-620 cm^{-1} spectral range is reported in Figure 6. This range is assigned to the vibration of υ2 and υ4 PO_4^{3-} bending modes. It was reported by S. Elgharbi and H. Lefires when they work about Tunisian phosphate rock that the Raman bands at 582, 591 and 607 cm^{-1} are assigned to υ4 PO_4^{3-} and the bands at 431 and 435 cm^{-1} are due to the υ2 PO_4^{3-} [12,13]. Then, the work reported by Karampasa about calcium phosphate confirmed very well the results above [29].

The Raman spectrum over the 850-1200 cm^{-1} range is reported in Figure 6. Similar intensity bands are found at 1056, 1100, 1116 cm^{-1} which are assigned to υ3 PO_4^{3-} antisymmetric stretching vibration, the three bandes are attributed to a pure fluorapatite [18]. Low intensity Raman band at 1009 cm^{-1} is attributed to υ1 PO_4^{3-} symmetric stretching mode [28,33,34].

From Raman analysis, we can conclude that the gettereing process in necessary to eliminate the impurities and organic matters which

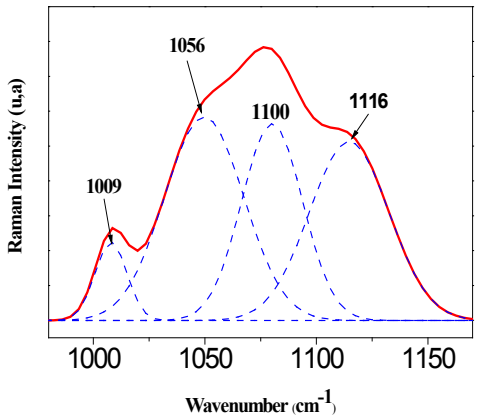

Figure 5: Raman spectrum of treated phosphate over the 850 cm^{-1}-1200 cm^{-1} spectral range.

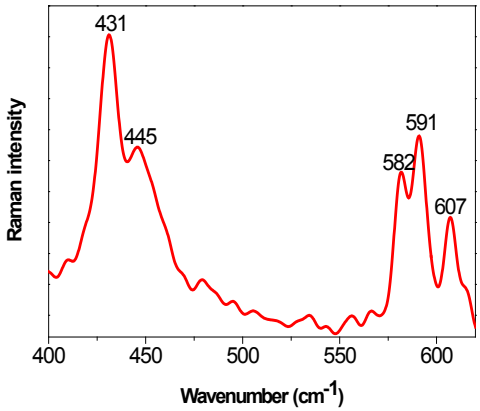

Figure 6: Raman spectrum of treated phosphate over the 400 cm^{-1} -620 cm^{-1} spectral range.

are the main causes of overlopped in reference phosphate rock, and consequently improves the structural properties.

TEM-EDAX characterization

The change in the physical structure of the treated sample in comparison with the raw ore was investigated by TEM. This scanning procedure consisted of looking for structure alterations, agglutination, porosity, morphology, compaction, and distribution, with qualitative and semi quantitative identification of elements [35].

It is shown in Figure 7 that the phosphate rock consists of two different particule phases with estimated sizes of 60 µm. Moreover, these phases are defined with tow portions which can be due to the accumulation of the impurities which escape the dispersion of the particles. The portion in light grey is formed by phosphorous rich components whereas the portion in dark grey are formed by calcium-rich components, which can be defined as $CaCO_3$, based on chemical analysis. No phosphorous was found in the carbonate parts. Carbonate-fluorapatite existing in the ore has only been observed in the parts with phosphorous-rich components. The surfaces of the parts with phosphate exhibit a compact structure with only little porosity.

The TEM micrographs of the treated sample by gettering process (porous phosphate treated 45 min at 900°C and eatching in mixture acid) is given in Figure 8 shows that the TP sample is formed by many crystals with baton forms. It seems that the RP sample was subdivided to many particles with different sizes. It was determined that the shrinkage and the cracks at the surrounding parts with phosphate occurring due to thermal and etching treatments [36]. The holes on the surfaces of the parts with phosphate prove that carbonate–fluorapatite was calcined and that the carbonate–fluorapatite changed to fluorapatite. This is due to the disappearance of the impurities which occupied interstitial sites, grain boundaries. Only the preponderant elements appear in the imagery which is confirmed by quantitative analysis. These results are in good agreement with the XRD analysis.

To get more insight of the composition of the RP and TP samples, Energy-dispersive X-ray (EDX) was used in many places of the sample area. The results were summarized in Table 1. From Figures 7 and 8, we noticed that the major elements before treatment are P, Ca, F in addition to the impurities such as Al, Si, S, Na, Mg…Whereas, after treatment only the P, Ca, F are presented with small traces S, Na and Si.

Table 1 shows the quantitative chemical composition. The analysis shows a homogeneous phase composed by P, Ca and F as being major elements consists mainly of fluorapatite. The chemical composition of phosphate rock shows that after treatement process, it changes to a rather poor in magnesium, in silica and metal such as Al, Fe.

Moreover, the electron microprobe analysis of samples allows us to

Element	RP	TP
Ca	26.27	49.03
P	10.92	28.8
F	3.4	13.43
Si	37.62	7.73
Al	9.08	1.53
Mg	8.87	1.85
Fe	2.31	0.06
S	1.38	0.51
Na	1.12	0.06
K	0.28	0.07
Ca/P	2.4	1.7

Table 1: Atomic percent of reference phosphate (RP) and treated phosphate (TP).

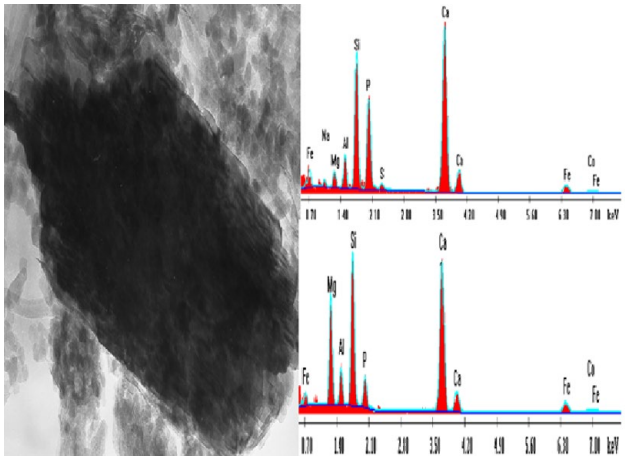

Figure 7: TEM and EDX analysis of reference phosphate rock.

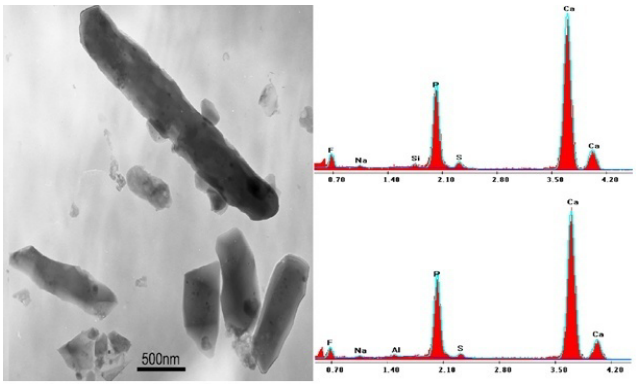

Figure 8: TEM and EDX analysis of Tunisian phosphate rock after treatment.

evaluate the ratio Ca/P. Compared to the reference phosphate are 2.4, treated phosphate (TP) is become 1.7 which is closer to the theoretical Ca/P molar ratio of pure FAP: 1.67. However, this proves the presence of carbonate-FAP and calcite in reference sample and the presence of calcium oxide in excess [28]. This difference in composition may take place by incorporation of ion present in the site of PO_4^{2-} group. In our case these elements are F^-, Na^+, CO_3^{2-} known to be incorporated into the network of the apatite.

Conclusion

A marked change on the properties of Tunisian phosphate rock was observed following the gettering process. The experimental results in this study suggest a significant improvement in the structure as well as the composition of the treated phosphate rock. Therefore, we consider that gettering process is not only a promising way to eliminate the impurities but also it enhances the use of phosphate rock in many fields.

References

1. Popescu IC, Filip P, Humelnicu D, Humelnicu I, Scott TB, et al. (2013) Removal of uranium (VI) from aqueous systems by nanoscalezero-valent iron particles suspended in carboxy-methyl cellulose. Journal of Nuclear Materials 443: 250-255.
2. Cevik U, Baltas H, Tabak A, Damla N (2010) Radiological and chemical assessment of phosphate rocks in some countries. Journal of Hazardous Materials 182: 531-535.
3. Zendah H, Khattech I, Jemal M (2013) Thermochemical and kinetic studies of the acid attack of "B" type carbonate fluorapatites at different temperatures (25-55°C). Thermochemica Acta 565: 46-51.
4. Mar SS, Okazaki M (2012) Investigation of Cd contents in several phosphate rocks used for the production of fertilizer. Microchemical Journal 104: 17-21.
5. Silva EF, Mlayah A, Gomes C, Noronha F, Charef A, et al. (2010) Heavy elements in the phosphorite from KalaatKhasba mine (North-western Tunisia): Potential implications on the environment and human health. Hazardous Materials 182: 232-245.
6. Guoa Z, Fanb J, Zhanga J, Kanga Y, Liua H, et al. (2015) Sorption heavy metal ions by activated carbons with well-developed microporosity and amino groups derived from Phragmites australis by ammonium phosphates activation. Journal of the Taiwan Institute of Chemical Engineers.
7. Marouan K, Messaoud H, Hatem E (2012) Purification of silicon powder by the formation of thin porous layer followed byphoto-thermal annealing. Nanoscale Research Letters 7: 444.
8. Koleva V, Petkova V (2012) IR spectroscopic study of high energy activated Tunisian phosphorite. Vibrational Spectroscopy 58: 125-132.
9. Garnit H, Bouhlel S, Baraca D, Chtara C (2012) Application of LA-ICP-MS to sedimentary phosphaticparticules from Tunisian phosphorite deposits: Insights from trace elemnts and REE into paleo-depositionelenvirenments. Chemie der Erde 72: 127-139.
10. Bachoua H, Othmani M, Coppel Y, Fatteh N, Debbabi M, et al. (2014) Structural and thermal investigations of a Tunisian natural phosphate rock. J Mater Environ Sci 5: 1152-1159.
11. Galai H, Sliman F (1994) Mineral characterization of the Oum El Khachebphosphorites.
12. Amini R, Vakili H, Ramezanzadeh B (2015) Studying the effects of poly (vinyl) alcohol on the morphology and anti-corrosion performance of phosphate coating applied on steel surface. Journal of the Taiwan Institute of Chemical Engineers.
13. Frost RL, Scholz R, Lopées A, Xi Y, Gobac ZZ (2013) Raman and infrared spectroscopic characterization of the phosphate mineral paravauxite $Fe^{2+}Al_2(OH)_2.8H_2O$. Spectrochimica Acta A Molecular and Biomolecular Spectrocopy 116: 491-496.
14. Elgharbi S, Horchani-Naifer K, Ferid M (2015) Investigation of the structural and mineralogical changes of Tunisian phosphorite during calcinations. J Therm Anal Calorim 119: 265-271.
15. Lefires H, Medini H, Megriche A, Mgaidi A (2014) Dissolution of Calcareous Phosphate Rock from Gafsa (Tunisia) Using Dilute Phosphoric Acid Solution. International Journal of Nonferrous Metallurgy 3: 1-7.
16. Guo F, Li J (2010) Separation strategies for Jordanian phosphate rock with siliceous and calcareous gangues. International Journal of Mineral Processing 97: 74-78.
17. Fleet ME (2009) Infrared spectra of carbonate apatites: υ_2-Region bands. Biomaterials 30: 1473-1481.
18. Antonakosa A, Liarokapis E, Leventouri T (2007) Theodora Leventouri, Micro-Raman and FTIR studies of synthetic and natural apatites. Biomaterials 28: 3043-3054.
19. Farmer VC (1974) The layer silicates. Mineralogical Society of London.
20. Incee DE, Johnston CT, Moudgil BM (1991) Fourier transformation infared spectroscopy study of adsorption of oleic acid on surfaces of apatite. J Angmuir 7: 1453-1457.
21. Wei W, Cui J, Wei Z (2014) Effects of low molecular weight organic acids on the immobilization of aqueous Pb(II) using phosphate rock and different crystallized hydroxyapatite. Chemosphere 105: 14-23.
22. Kolevo V, Stevo V (2013) Phosphate ion vibrations in dihydrogen phosphate salts of the type $M(H_2PO_4)_2 \cdot 2H_2O$ (M = Mg, Mn, Co, Ni, Zn, Cd): Spectra–structure correlations. Vibrational Spectroscopy 64: 89-100.
23. Fahamin A, Nasiri-Tabrizi B, Ebrahimi-Kahrizsangi R (2012) Synthesis of calcium phosphate-based composite nanopowders by mechanochemical process and subsequent thermal treatment. Ceramics International 38: 6729-6738.
24. Zafar ZI, Ashraf M (2007) Selective leaching kinetics of calcareous phosphate rock in lactic acid. Chemical Engineering Journal 131: 41-48.
25. Sheng Q, Sheng V, Liu S, Li W, Wang L, Tang C (2013) Enhanced broad band near-infrared luminescence and peak wavelength shit of Yb-Bi ions co-doped phosphate glasses containing. Journal of Luminescence 144: 26-29.
26. Wenyuan YU, Guanlai LI, Li Z (2010) Sonochemical synthesis and photoluminescence properties of rare-earth phosphate core/shell nanorods. Journal of Rare Earths 28: 171-175.
27. Babu SS, Babu P, Jayasankar CK, Sievers W, TroSter T, et al. (2007) Optical absorption and photoluminescence studies of Eu3+-doped phosphate and fluorophosphate glasses. Journal of Luminescence 126: 109-120.
28. Bandara AMTS, Senanayake G (2015) Leachability of rare-earth, calcium and minor metal ions from natural fluoropatite in perchloric, hydrochloric, nitric and phosphoric acid solutions: Effect of proton activity and anion participation. Hydrometallurgy 153: 179-189.
29. Karampasa IA, Kontoyannis CG (2013) Characterization of calcium phosphates mixtures. Vibrational Spectroscopy 64: 126-133.
30. Nakamoto K (2009) Infrared and Raman spectra of inorganic and coordination compounds: part A: Theory and applications in inorganic chemistry (6th edn.). John Wiley & Sons inc, USA.

31. Williams Q, Knittle E (1996) Infrared and Raman spectra of $Ca_5(PO_4)3F_2$-fluorapatite at high pressures: compression-induced changes in phosphate site and Davydov splitting. J Phys Chem Solids 57: 417-422.

32. Bushiri MJ, Jayasree RS, Fakhfakh M, Nayar VU (2002) Raman and infrared spectral analysis of thallium niobyl phosphates: $Tl_2NbO_2PO_4$, $Tl_3NaNb_4O_9(PO_4)_2$ and $TlNbOP_2O_7$. Materials Chemistry and Physics 73: 179-185.

33. Frost RL, Lopez A, Scholz R, Xi Y, Belotti FM (2013) Infrared and Raman spectroscopic characterization of the carbonate mineral huanghoite and in comparison with selected rare earth carbonate. Journal of Molecular Structure 1051: 221-225.

34. Frost RL, López A, Xi Y, Cardoso LH, Scholz R (2014) A vibrational spectroscopic study of the phosphate mineral minyuliteKAl$_2$(OH,F)(PO$_4$)$_2$4(H$_2$O) and in comparison with wardite. Spectrochimica Acta A Molecular and Biomolecular Spectroscopy 124: 34-39.

35. Francisco EAB, Prochnow LI, Motta de Toledo MC, Ferrari VC, Luís de Jesus S (2007) Thermal Treatment Of Aluminous Phosphates Of The Crandallite Group And Its Effect On Phosphorus Solubility. Sci Agric 64: 269-274.

36. Özer AK, Gülaboglu MS, Bayrakçeken S, Weisweiler W (2006) Changes in physical structure and chemical compositionof phosphate rock during calcination in fluidizedand fixed beds. Advanced Powder Technol 17: 481-494.